

# Synchrotron X-ray footprinting on tour

Jen Bohon,<sup>a,b\*</sup> Rhijuta D'Mello,<sup>a,b</sup> Corie Ralston,<sup>c</sup> Sayan Gupta<sup>c</sup> and Mark R. Chance<sup>a,b</sup>

Received 24 June 2013  
Accepted 4 September 2013

<sup>a</sup>Center for Synchrotron Biosciences, Case Western Reserve University, National Synchrotron Light Source, Brookhaven National Laboratory, Upton, NY 11973, USA, <sup>b</sup>Center for Proteomics and Bioinformatics, Case Western Reserve University, 10900 Euclid Avenue, Cleveland, OH 44106, USA, and <sup>c</sup>Berkeley Center for Structural Biology, Physical Biosciences Division, Lawrence Berkeley National Laboratory, 1 Cyclotron Road, Berkeley, CA 94720, USA. \*E-mail: jbohon@bnl.gov

Synchrotron footprinting is a valuable technique in structural biology for understanding macromolecular solution-state structure and dynamics of proteins and nucleic acids. Although an extremely powerful tool, there is currently only a single facility in the USA, the X28C beamline at the National Synchrotron Light Source (NSLS), dedicated to providing infrastructure, technology development and support for these studies. The high flux density of the focused white beam and variety of specialized exposure environments available at X28C enables footprinting of highly complex biological systems; however, it is likely that a significant fraction of interesting experiments could be performed at unspecialized facilities. In an effort to investigate the viability of a beamline-flexible footprinting program, a standard sample was taken on tour around the nation to be exposed at several US synchrotrons. This work describes how a relatively simple and transportable apparatus can allow beamlines at the NSLS, CHESS, APS and ALS to be used for synchrotron footprinting in a general user mode that can provide useful results.

© 2014 International Union of Crystallography

**Keywords:** structural biology; footprinting; X-rays; beamlines; radiolysis.

## 1. Introduction

X-ray-based synchrotron footprinting is used to study solution-state structure and dynamics of biological macromolecules. This technology employs X-ray beams produced by synchrotron radiation to generate hydroxyl radicals in solution on the microsecond to millisecond timescales appropriate for probing macromolecular dynamics (including for DNA, RNA and proteins) while minimizing sample perturbation. Macromolecules in solution have vastly lower concentrations than the solvent such that X-rays target bulk water efficiently compared with interacting with the macromolecule directly. X-rays of suitable energies can deposit considerable energy in water, resulting in excitation and fragmentation of water with a high yield of hydroxyl radicals (2.87 per 100 eV; Ralston *et al.*, 2000) that diffuse isotropically in solvent and covalently modify solvent accessible targets. Exposure of samples to X-rays is typically accomplished either *via* electronic shutter (~10 ms minimum exposure) or *via* rate of flow of sample through the beam, which allows shorter exposures but requires more sample.

The encounter of solvent-derived hydroxyl radicals with nucleic acids results in efficient cleavage of the phosphodiester backbone while hydrogen abstraction or other reactions with amino acid side-chains can result in stable covalent modifi-

cations in proteins (Gupta *et al.*, 2007; Xu & Chance, 2007). In structural regions of macromolecules where they are folded, bind a ligand and form an interface or change conformation in other ways that change the accessibility of bulk solvent, the susceptible sites in the macromolecule change their rate and extent of reaction with radicals. These changes in reactivity reveal information about the macromolecule's solvent accessibility with high resolution. For nucleic acids, one analyzes the pattern of fragments after X-ray exposure by gel electrophoresis using an end-label; the sequencing ladder produced is analyzed for the 'protected sections' (that are not cleaved) yielding a 'footprint' (Brenowitz *et al.*, 2002). For proteins, exposed samples are digested with proteases and analyzed using mass spectrometry to determine the extent and sites of modification (Guan *et al.*, 2004; Kiselar *et al.*, 2002; Maleknia *et al.*, 1999; Takamoto & Chance, 2006). The data provide detailed structural information at the single nucleotide and single side-chain level that can be used to map local structure as well as regions of macromolecular interaction, which can subsequently become constraints for molecular modeling to generate high-resolution structures (Kamal & Chance, 2008; Takamoto *et al.*, 2007). The X-ray dose required to conduct nucleic acid (cleavage) and protein (modification) X-ray footprinting experiments is similar, thus the comparisons of beamlines made in this paper are relevant to both approaches.

The techniques have been extensively reviewed in the literature, including both review articles and original research, and have become well accepted as part of the toolkit for modern molecular biophysics research.

Footprinting is exceptionally complementary (and powerful) in the context of parallel X-ray crystallography studies, which can provide high-resolution structural information about components of complexes, and small-angle X-ray solution scattering and cryo-electron microscopy studies, which can provide ‘global’ molecular envelopes within which the local structural information from footprinting can be better understood (Shi *et al.*, 2010; Chaudhuri *et al.*, 2011). In particular, synchrotron footprinting provides ‘local’ structural information in solution for gaining insight into dynamic processes, including those involving large RNA–protein and protein–protein assemblies, on biologically relevant timescales and under physiological conditions (Brenowitz *et al.*, 2002, 2005; Nguyenle *et al.*, 2006; Adilakshmi *et al.*, 2006a, 2008).

For more than a decade now, synchrotron-based footprinting studies at the NSLS X28C beamline, constructed and operated by the Center for Synchrotron Biosciences (<http://csb.case.edu/>), have provided unique insights and approaches for time-resolved studies of macromolecular dynamics (Deras *et al.*, 2000; Dhavan *et al.*, 2002; Nguyenle *et al.*, 2006; Sclavi *et al.*, 1997, 1998a,b; Shcherbakova *et al.*, 2004; Uchida *et al.*, 2003), for examining the structure of large macromolecular assemblies (Guan *et al.*, 2004, 2005; Bohon *et al.*, 2008; Jennings *et al.*, 2008; Kamal *et al.*, 2007; Kiselar *et al.*, 2003a,b, 2007) and membrane proteins (Angel *et al.*, 2009; Gupta *et al.*, 2010), and even for *in vivo* studies of macromolecules (Adilakshmi *et al.*, 2006b, 2009). Currently, over 115 user publications have been deposited at <https://pass.nsls.bnl.gov/publications/search.asp> (search by beamline, X28C).

With the upcoming shutdown of the NSLS in 2014, the X28C beamline will no longer be available. Although a new specialized facility for footprinting will be constructed at the NSLS-II as rapidly as possible, for the science to continue uninterrupted, footprinting programs must be pursued at other synchrotron facilities. Fortunately, footprinting is relatively unique as a synchrotron technique in that no detector or associated data collection infrastructure is required at the beamline. The beamline requirements are simple: broadband (most efficient in the 5–20 keV range), high flux density X-rays in a spot size which can accommodate the vertical size of a capillary [current standard is 0.7 mm internal diameter (ID)] within the relatively uniform portion of the beam, and a space at the end of the beampipe to place the apparatus. With varying levels of capability, a number of beamlines at synchrotrons around the country can meet these requirements. These facilities can be accessed using ‘general user’ time through the standard mechanisms provided for use of these government-funded resources. In this work, we explored the ability of a range of facilities to accommodate successful footprinting experiments; we also examined the effects of the varying flux densities available in various beamline configurations on the signal-to-noise of footprinting data. Demonstration of flux density as a key figure of merit for X-ray

footprinting provides important design guidance for future beamline development. In addition, based on the results of the tests performed in this work, a new exploratory synchrotron footprinting program is currently being established at the Advanced Light Source. Initially, this program will make use of beamlines 5.3.1 and 3.2.1 on an as-needed basis in order to accommodate both new X-ray footprinting users and to maintain user programs currently in progress at the NSLS footprinting center. In parallel, ALS beamline 3.3.1 will be recommissioned in 2014 and will be a dedicated X-ray footprinting program in order to increase access to this simple and powerful structural biology technique. In summary, synchrotron X-ray footprinting can be easily performed at facilities across the USA and facilities dedicated to conducting such experiments are growing and will be improved over the next few years.

## 2. Methods

### 2.1. Exposure apparatus

The capillary X-ray exposure flow cell in the mount (Fig. 1) was constructed at the Case Western Reserve University Center for Synchrotron Biosciences. For the flow cell, a 0.7 mm ID fused silica tubing standard in HPLC use (TSP700850 Polymicro Technologies) was mounted on each end to 1.575 mm ID PVC tubing (Lee Fluid Control) with brief application of a heat gun to ensure a complete seal. A Luer-lock fitting was used on the input side to securely affix the tubing to the injection syringe; no termination was required on the output. A stainless-steel frame was machined to mount and protect the capillary flow cell; this apparatus also includes a horizontal slit assembly for beam width definition and a diode mount to facilitate alignment of the capillary in the beam path. The width of the slit and the speed of flow of the sample determine the exposure time for the sample. For these experiments, a syringe pump (Harvard model ‘33’) was mounted with 5 ml plastic syringes to feed liquid samples through the exposure cell into a sample tube for collection. For most experiments, a 4 mm horizontal slit width was used to enable exposure times down to 10 ms within the maximum

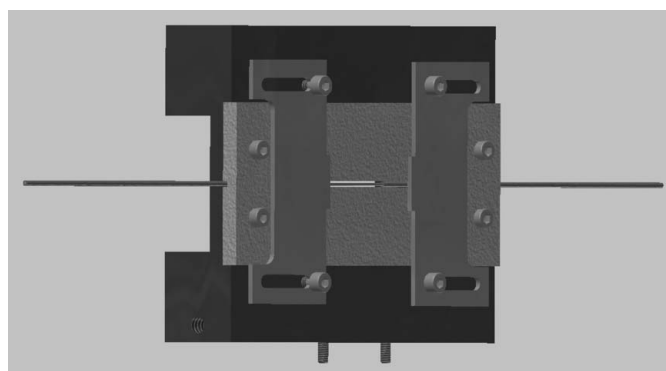


**Figure 1**  
Capillary flow cell in mount.

speed of the pump (smaller slit sizes will allow shorter exposures). A laptop was used to control the liquid flow from outside of the experimental hutch *via* a standard serial and USB connection using Hyperterminal. This basic flow cell apparatus was used for all experiments.

### 2.2. Beamline descriptions

Although the basic flow cell apparatus used for these experiments was identical, each beamline used has unique characteristics and configurations. However, there are a few similarities for two sets of beamlines. For the white-beam beamlines with focusing or collimating optics (NSLS X28C, ALS 5.3.1 and CHESS A2), the stainless-steel slits are sufficient for beam definition on the sample due to filtering out of the high-energy X-ray spectrum *via* use of a mirror. These beamlines provide the highest flux-density beams, considered optimal for synchrotron footprinting, in a variety of shapes and sizes that vary with the adjustable mirror parameters. The resulting beams can be focused to precisely the proper size for the sample to enhance the flux density, but require care to be taken to create a relatively uniform beam (most important to be uniform perpendicular to the flow direction). Motorized alignment with an in-line diagnostic is necessary to properly position the sample cell in the beam. The white-beam beamlines without focusing optics (APS 10-BM-A, ALS 8.3.2 and ALS 3.2.1) require additional lead shielding added to the slits or use of white-beam slits provided separately by the beamlines to properly define the beam on the sample. These beamlines provide rather large, relatively uniform beams within which it is easy to align a capillary; however, all alignment for these beams was performed manually (using burn paper or diodes and iterative motion). Typical footprinting experiments (Gupta *et al.*, 2007) involve either flow through an exposure cell or capillary or exposure of a small volume sample held by surface tension in the bottom of a microcentrifuge or PCR tube. Thus two beam sizes/morphologies are desirable: a rectangular beam slightly larger in the vertical than the flow cell (commonly <1 mm diameter) but with several millimeters of potential horizontal beam to increase exposure without slowing the flow too much, and a relatively round beam slightly larger than the sample droplet in the bottom of the tube (~2.5 mm for 5  $\mu$ l in a PCR tube). Specifics on the beamlines and notable differences are described below.

NSLS beamline X28C is specifically configured and optimized for performing synchrotron footprinting experiments in a variety of environments. In addition to the syringe pump, apparatus is available for temperature control during exposure, for steady-state small-volume sample exposure (few  $\mu$ l) (243–318 K) or larger volumes in a KinTek quench-flow (~273–318 K) which can also accommodate rapid mixing for time-resolved experiments. An in-line fraction collector is available for continuous-flow experiments. Beamline X28C is located on a bending-magnet source and is equipped with a Pd-coated toroidal focusing mirror. The beamline is capable of providing up to nearly 90 W mm<sup>-2</sup> (measured *via* calorimetry)

into a spot size as small as 500  $\mu$ m  $\times$  500  $\mu$ m (Sullivan *et al.*, 2008). For these experiments, the mirror was adjusted to create a beam with FWHM of ~800  $\mu$ m  $\times$  6 mm in the vertical and horizontal dimensions, respectively. To create the conditions conducive for useful exposure of cytochrome *c*, the dose in the sample was reduced by the addition of 380  $\mu$ m of aluminium attenuation (to use the additional power available for this simple sample, more rapid exposure times would need to be used than were easily accessible with the portable syringe pump apparatus used in these experiments).

APS beamline 10-BM-A is located on a bending-magnet source and generally provides white/pink beam for X-ray lithography, photochemistry and high-energy tomography of large objects. The beam can be up to 6 mm (V)  $\times$  110 mm (H) and is quite uniform over the size of the capillary within that area. White-beam slits are available at the beamline and significant external motor control (several axes) makes alignment simple. A relatively large area can be opened right at the end of the beampipe to set up a footprinting apparatus by simply moving the standard set-up out of the way *via* motor control systems already integrated into the beamline.

CHESS beamline A2 receives half of the beam passing through a 49-pole wiggler source and is equipped with a rhodium-coated vertically collimating mirror (3.5 mrad minimum allowed angle). A2 beamline science is generally focused on diffraction-based materials science and solid-state physics; the monochromator that services these typical experiments is retractable to provide a pink beam in the hutch, but does require 8 h of beamline downtime both to retract and to replace for vacuum maintenance. The white-beam slits are located upstream of the mirror and were set to 1 mm (V)  $\times$  4 mm (H) for this work. The X-ray beam is estimated to provide 10 W mm<sup>-2</sup> for sample exposure and is approximately Gaussian in shape over the vertical dimension. The beamline is equipped with an optical table that can be completely cleared for placement of experimental apparatus and has appropriate motor controls for sample alignment integrated into the beamline systems.

ALS beamline 5.0.2 utilizes a wiggler insertion device and is exclusively used in conjunction with a monochromator; this beamline is generally used for macromolecular crystallography. For the footprinting experiments shown in this work, the monochromator was set to produce 11 keV photons. Measurements taken at 8 keV did not produce significantly different results (data not shown). The beamline is capable of providing of the order of  $2 \times 10^{13}$  photons s<sup>-1</sup> into a beam spot of 250  $\mu$ m  $\times$  600  $\mu$ m at this energy; however, in order to obtain a usable beam size (~1 mm  $\times$  5.5 mm), the experiment was moved several meters back from the focal point onto a roll-in cart to which the apparatus was clamped. An ~3 m PVC rough-vacuum flight tube capped with Kapton was constructed and installed for this experiment to reduce the air path. All motor control was manual; alignment was performed using burn paper.

ALS beamline 8.3.2 is a white-beam beamline located on a superbend source; the beamline is generally used for hard X-ray microtomography and provides the unusual capability

to observe the fluid flowing through the capillary during the experiment (Fig. S2<sup>1</sup>) using the remaining transmitted X-rays with a Cooke PCO4000 CCD with scintillator. The beam size is  $\sim 5$  mm  $\times$  35 mm at the sample position.

ALS beamline 3.2.1 is located on a bending-magnet source and is used for commercial deep-etch lithography. This beamline is located closer to the source than 8.3.2, making the flux density somewhat similar between the beamlines despite the superior source properties of the superbend. The beam size at the sample position is  $\sim 10$  mm  $\times$  100 mm. The apparatus set-up at the beamline is shown in Fig. S3. This beamline is not currently available for general users and was made available specifically for this experiment to the authors. Beam time will be made available for X-ray footprinting users as part of the new footprinting program at the ALS.

ALS beamline 5.3.1 is located on a bending-magnet source, and is equipped with a platinum-coated toroidal focusing mirror. It is estimated to be capable of providing  $1.5 \times 10^{16}$  photons  $s^{-1}$  into as small as a 250  $\mu\text{m} \times 60 \mu\text{m}$  beam. This beamline is substantially similar to NSLS X28C in its optical configuration and usable flux density, and thus has significant potential as a location for a footprinting program. Improved usable flux density is expected as development of the sample-handling system evolves to take advantage of the fully focused beam. This beamline is not currently available for general users and was made available specifically for this experiment to the authors. Beam time will be made available for X-ray footprinting users as part of the new footprinting program at the ALS.

Future use of beamlines 3.2.1 and 5.3.1 has been negotiated with the Experimental Systems group at the ALS in order to establish an exploratory footprinting program at the ALS. These beamlines will be available as needed to support displaced NSLS footprinting users, as well as to establish new collaborations for structural biology studies. In parallel, permission has been granted by the ALS to open the previously decommissioned beamline 3.3.1 for the sole purpose of developing an X-ray footprinting program. Beamline 3.3.1 shares the white-light bending-magnet source with 3.2.1, and funds are actively being pursued to purchase a Pt-coated toroidal focusing mirror to be installed outside the shield wall, centered at 11.1 m (two-thirds of the distance) from the source. We anticipate that the focusable beam along with the use of microfluidic sample flow at 3.3.1 will enable a usable flux density at the sample comparable with beamline 5.3.1, and will therefore be suitable for continuation of X-ray footprinting studies both before and after the completion of the NSLS-II footprinting beamline.

**Table 1**

Comparative parameters for various synchrotron beamlines.

Facility	Beamline	Ring current (mA)/energy (GeV)	Source	Optics	Rate constant ( $s^{-1}$ )
NSLS	X28C	292/2.8	Bending magnet	Toroidal mirror	2034 <sup>†</sup>
ALS	5.3.1	500/1.9	Bending magnet	Toroidal mirror	1726 <sup>†</sup>
CHES	A2	186/5.3	Wiggler (half)	Vertical collimating mirror	337
APS	10-BM-A	102/7.0	Bending magnet	–	205
ALS	8.3.2	500/1.9	Superbend	–	71
ALS	3.2.1	500/1.9	Bending magnet	–	55
ALS	5.0.2	500/1.9	Wiggler	Monochromator (11 keV)	4

<sup>†</sup> Rates stated are a minimum value; the actual rate is likely to be higher, but measurement was outside the range of sensitivity past initial data points.

### 2.3. Samples

For comparison of beamline capabilities, samples containing only 10 mM of either sodium phosphate or sodium cacodylate buffer and 1–5  $\mu\text{M}$  Alexa 488 fluorescent dye (Invitrogen) were exposed to the X-ray beam. A hand-held Turner Biosystems TBS-380 fluorimeter was used to observe the rate of reduction in fluorescence in the samples for a series of four exposure times (Fig. 2) (Gupta *et al.*, 2007). The loss of intensity is fit to a single exponential function providing an apparent rate of Alexa modification. This rate is a proxy for the available OH radical dose and also the X-ray flux density. Protein samples consisted of 10  $\mu\text{M}$  horse heart cytochrome *c* (Sigma-Aldrich) in 10 mM phosphate buffer 50 mM NaCl, pH 7–8. For a direct comparison of the effective dose in each protein sample, calibration samples which contained 1–5  $\mu\text{M}$  Alexa 488 fluorescent dye (Invitrogen) in addition to the protein were used (Fig. S1, Table S1). Between different protein samples, the tubing was cleaned out with ethanol and water. Each protein sample was collected into a tube

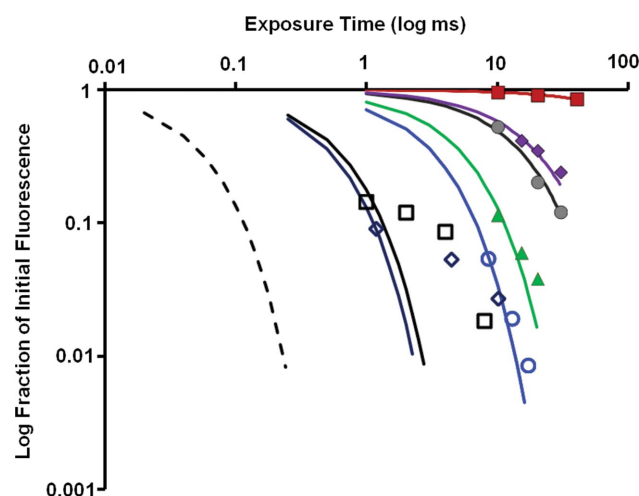


**Figure 2**

Dose-response curves for maximal available dose at various synchrotron beamlines (rates listed in Table 1). Increased dose on the sample quenches the fluorescence of the fluorophore dye. Filled red squares: ALS 5.0.2; filled purple diamonds: ALS 3.2.1; filled grey circles: ALS 8.3.2; filled green triangles: APS 10-BM-A; open blue circles: CHES A2; open black squares: ALS 5.3.1; open navy diamonds: NSLS X28C; dotted line: NSLS-II XFP (estimate).

<sup>1</sup> Supporting data for this paper are available from the IUCr electronic archives (Reference: RV5004).

containing methionine amide to quench secondary reactions, then flash frozen in liquid nitrogen and stored on dry ice for shipping. At least four exposure times were collected for each sample to establish a modification rate.

### 2.4. Sample processing and analysis

Proteolytic digestion of cytochrome *c* was carried out using standard methods with trypsin enzyme (Promega) overnight digestion at 310 K at pH 8 in 50 mM ammonium bicarbonate buffer. The tryptic digest of cytochrome *c* was analyzed using a Thermo-Fisher LCQ DecaXP Plus mass spectrometer interfaced with a Waters Alliance 2695 HPLC according to standard LC-ESI-MS protocols. LC-MS/MS parameters were set for carrying out a full data-dependent scan for OH radical modifications. MS/MS spectra for the unmodified and modified peptides were manually interpreted with the aid of the *ProteinProspector* (University of California, San Francisco) algorithm and *Bioworks* 3.3 software. Selected ion chromatograms from the LC-ESI-MS results were used to quantify the extent of modification. The fraction unmodified for each peptide (or separate probe residue peak, where applicable) from the chromatogram was calculated as the ratio of area under the peak curve of the unmodified peptide to the sum of integrated peak areas from the modified and unmodified peptides. The dose-response curve (fraction unmodified *versus* X-ray irradiation time) was fitted to a first-order exponential decay function with Microsoft Excel *via* least-squares minimization to determine the modification rate constants.

## 3. Results

### 3.1. Beamline comparison

Despite the significant differences in beamline capabilities and configurations, data were successfully collected at all facilities tested. Source properties and beamline optics for each beamline tested are listed in Table 1. In addition to exposure and full footprinting analysis of the benchmark protein cytochrome *c*, each beamline was tested for comparative maximal available dose rate using the fluorescent dye Alexa 488 as a marker (Gupta *et al.*, 2007), ease of facility access, ease of set-up, availability of support, and facilities for sample preparation.

Observation of performance of beamlines using the maximal available flux for the apparatus provided indicates a broad spectrum of capabilities (Fig. 2, Table 1). Focused white-light beamlines X28C at the NSLS and 5.3.1 at the ALS produce a significant dose of hydroxyl radicals with very short exposure times, quenching the fluorescent dye to below the sensitivity level of the fluorimeter after only a few milliseconds (causing deviation from the fit). The vertically collimated white beam at CHESS A2 provides about a sixfold lower response. Of the unfocused white-beam beamlines, APS beamline 10-BM-A provides a tenfold lower rate constant than the focused white-beam stations, and ALS beamlines 8.3.2 and 3.2.1 have 30- and 40-fold lower rates, respectively. ALS 5.0.2 is a monochromatic beamline, thus has significantly

less flux, and has a correspondingly  $\sim 500$ -fold lower response than the focused white-beam beamlines. The NSLS-II XFP beamline, anticipated to come online by 2016, is projected to provide at least an additional order of magnitude in flux density for X-ray footprinting experiments.

In general, all of the facilities provided a laboratory space separate from the beamline for full sample preparation and a smaller (but adequate) space at the beamline for simple procedures. In all cases, the dose-response assay using the fluorescent dye and hand-sized fluorimeter could be performed on-site at the beamline. Access to liquid nitrogen, desirable for some experiments, was also ubiquitous. Access to a 193 K freezer and acquisition of dry ice for sample storage and shipping was not convenient to the beamlines at APS 10-BM-A or at CHESS A2; however, the biology department of Argonne National Laboratory and the MacCHESS molecular diffraction facility at the CHESS (traveling to different buildings at both sites) were willing to provide what was needed. Dry ice was available at the ALS and the NSLS through beamline staff, and a 193 K freezer was accessible within the building in both cases. Aside from X28C, where footprinting is the standard experiment, experimental set-up did require significant beamline support from the local staff initially to place the flow cell and syringe pump in the proper position and to obtain the serial signal needed to operate the syringe pump out of the hutch. At the ALS and the CHESS, optical table accessories and similar parts were gathered by beamline staff for this purpose from a variety of locations. For APS 10-BM-A, the beamline staff rapidly machined the appropriate parts on-site to accommodate the experiment. The level of support was extremely strong in all cases and much of this set-up process can be streamlined going forward now that these pilot experiments have demonstrated what is needed.

Access to NSLS X28C was obtained through the participating research team system, as several of the authors are members of the beamline staff; however, it should be noted that X28C footprinting beam time is also available through the NSLS general user proposal system. Both APS 10-BM-A and CHESS A2 were accessed through the general user proposal systems at the respective facilities; the CHESS system specifically allowed access for this first experiment through a feasibility proposal. However, it should be noted that, because the focus of these beamlines is not biological in nature, a large number of footprinting experiments will likely not be supported there. Access to the ALS beamlines was provided through donation of beamline-staff beam time and coordinated through the Berkeley Physical Biosciences Division and the ALS. Two of the beamlines used, 3.2.1 and 5.3.1, are not generally available for outside users, except through the exploratory footprinting program which is currently under development at the ALS.

### 3.2. Footprinting of a benchmark sample

Cytochrome *c* is a well studied relatively small soluble protein, with a known structure and behavior in solution.

Cytochrome *c* has also been used in previous footprinting studies (Gupta *et al.*, 2012), thus the modification sites are known and the relative positions within the chromatogram identified. Because of this, cytochrome *c* was chosen as a benchmark, and full footprinting studies were performed using this protein at some of the various synchrotron facilities. Fig. 3 shows the raw modification rates observed for each modified cytochrome *c* amino acid and the rates corrected for differences in the beamlines using the Alexa 488 calibration data (Fig. S1, Table S1). The different flux densities used in the experiments create a clear hierarchy of modification rates (Fig. 3a); however, the comparative rates between probe residues within a given experiment are nearly identical. Note that the raw measured modification rates at the monochromatic beamline are so low as to be barely visible in the chart; however, with normalization (Fig. 3b) even these data are directly comparable with those from other beamlines. Normalizing in this manner does, of course, necessarily multiply the error associated with the low signal-to-noise data provided by the lower-flux beamlines, but the pattern of modification remains quite distinctive. Detailed data for

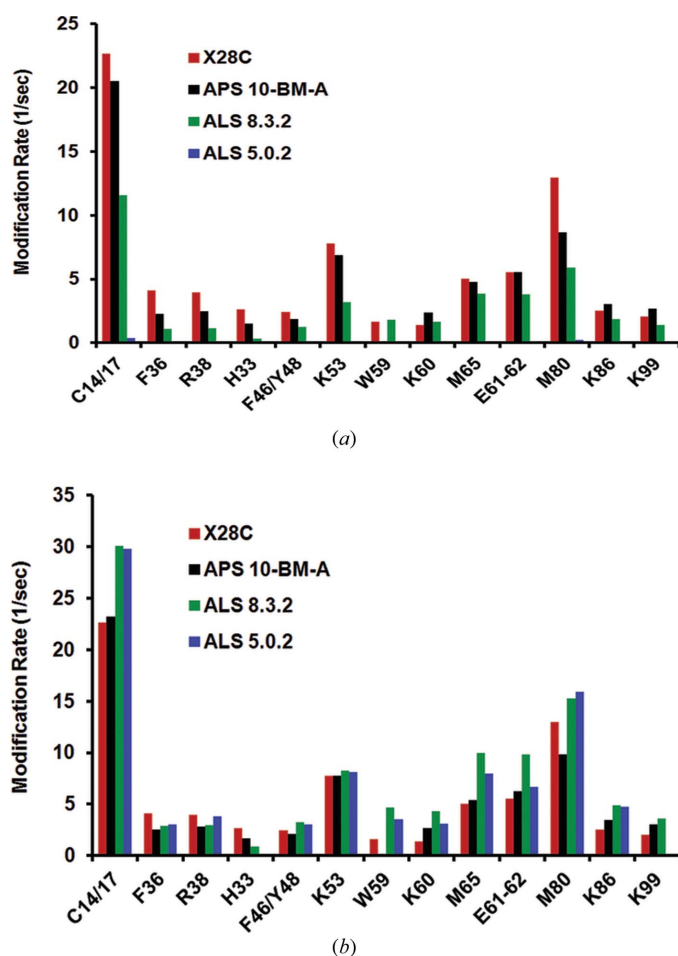


**Figure 3**  
Cytochrome *c* footprinting data comparison. (a) Raw modification rates for cytochrome *c* probe residues for each beamline tested. (b) Normalized modification rates using fluorophor calibration. Modification rate data are available in tabular format in the supporting information.

specific modification rates and sites on cytochrome *c* peptides for all experiments are provided in the supporting material (Tables S2 and S3).

### 3.3. Benefits of increased flux density

As the technique continues to develop, X-ray synchrotron footprinting is being applied to successively more complex biological systems, including studies of macromolecules in buffers which include significant concentrations of hydroxyl radical scavengers (Bohon *et al.*, 2008; Angel *et al.*, 2009) [or even samples *in vivo* (Adilakshmi *et al.*, 2006b, 2009)] and time-resolved studies which are demanding progressively shorter time scales. In order to overcome the scavenging effects of complex sample environments, the steady-state concentration of hydroxyl radicals must be increased (by increasing the X-ray flux density) or the sample must be exposed for longer times, maintaining the radical concentration over time to increase the opportunity for appropriate modification events to occur. Longer oxidation times increase the amount of secondary and tertiary radiolysis products (Ralston *et al.*, 2000), which contribute to chemical noise in the resultant LC-MS experiments. Therefore, it is far preferable to improve the flux density and decrease the necessary exposure time, both to gain access to shorter time scales for time-resolved experiments and also to improve the quality of the data obtained. An example of the effect of exposure time is seen in Fig. 4, in which chromatograms for two cytochrome *c* peptides from experiments performed at the NSLS X28C (10 ms exposure) and the ALS 8.3.2 (30 ms exposure) are compared. These samples were given approximately equivalent overall doses as observed from fluorophor calibration curves (~35% unmodified sample remaining, Fig. S1) over different exposure times. The signal-to-noise ratio decreases from two-fold to five-fold as the exposure time is increased in comparing the data from the NSLS with the ALS. The deterioration in signal-to-noise is clear in both the examination of the unmodified peptide as well as the modified (+16) oxidized species. This is important as both modified and unmodified species are quantified in typical experiments. For this example, although the modifications are still observable for the longer exposures, it is clear that additional decreases in the signal-to-noise ratio would result in completely obscured data (indistinguishable from the noise). This effect thwarted early attempts at studies of large macromolecular structures in scavenging buffers; these studies were only successful after increasing the X-ray flux density through installation of a focusing mirror at NSLS X28C (Bohon *et al.*, 2008; Jennings *et al.*, 2008). Experiences with complex systems such as these continues to drive the development of beamline instrumentation for X-ray footprinting, thus the next generation of beamline for these studies (the XFP facility at NSLS-II) will provide at least ten times higher flux density X-ray beams than are currently available. This will enable shorter exposures, making microsecond time-resolved studies feasible and will provide even higher signal-to-noise data for studies of more complex macromolecular systems.

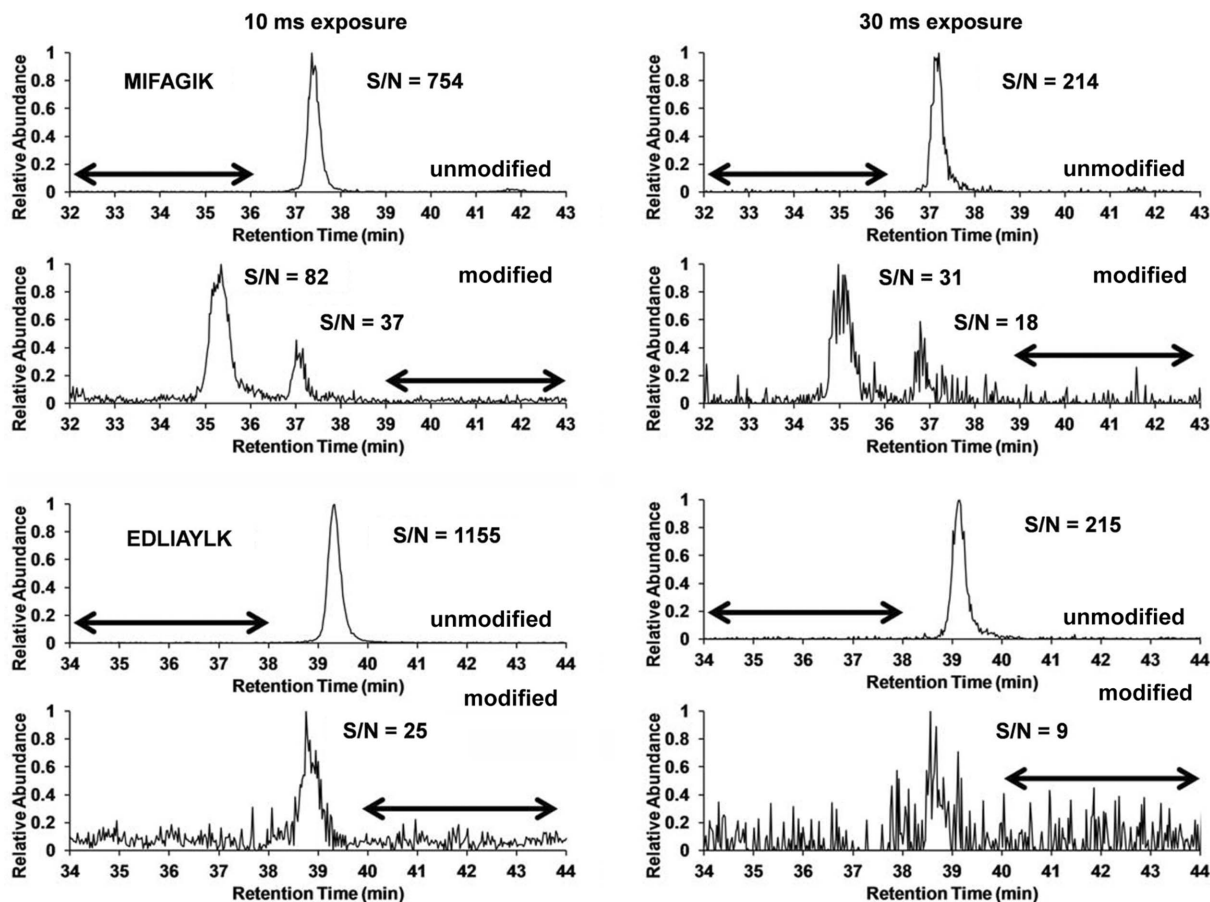


**Figure 4**  
 Comparison of data quality for different lengths of exposure with equivalent dose. NSLS X28C 10 ms exposure (left) and ALS 8.3.2 30 ms exposure (right) are shown for two cytochrome *c* peptides. Unmodified spectra (extraction of peptide mass) are shown above the corresponding modified spectra (extraction of peptide mass + 16 corresponding to one oxidation event). Arrows indicate regions over which r.m.s. noise was calculated. Note that the quality of the mass spectra due to sample processing and instrument sensitivity also strongly impact the signal-to-noise (S/N) ratio.

#### 4. Conclusions

These studies demonstrate that synchrotron facilities available at the NSLS, ALS, CHESS and APS are capable of supporting X-ray footprinting experiments utilizing a relatively simple and transportable apparatus. For a low-molecular-weight monomeric sample in a simple sample environment, data can be acquired at nearly any beamline and data of high quality can be acquired at any of the white/pink-beam stations investigated (or any similar beamlines elsewhere). For more complex samples, higher flux density is required to provide higher signal-to-noise data in a highly radical-scavenging environment; beamlines X28C at the NSLS or 5.3.1 at the ALS afford the highest flux density beams of those investigated; however, there is a considerable middle ground where the other white-beam stations still hold significant potential. Although it is expected that the new footprinting beamline being developed for NSLS-II will achieve even higher standards, this facility will not be available immediately. In addition to finding a temporary home for the X28C footprinting program, utilization of other facilities allows dissemination of the technology that can make a lasting impression. Synchrotron X-ray footprinting is a powerful structural biology tech-

nique that can be broadened significantly in accessibility by making programs available at multiple facilities around the USA.

The authors would like to thank Mike Sullivan, John Toomey and Don Abel for expert technical support at the NSLS X28C beamline and fabrication of the capillary flow cell and mount. The authors would also like to acknowledge Rich Celestre (ALS 5.3.1), John Katsoudas (APS 10-BM-A), Dula Parkinson (ALS 8.3.2) and Jacob Ruff (CHESS A2) for significant assistance with the experimental set-up at the denoted beamlines. Funding for this research was supported by the National Institute for Biomedical Imaging and Bioengineering under awards P30-EB-09998 and R01-EB-09688 and by the National Science Foundation under award DBI-1228549. Use of the National Synchrotron Light Source, Brookhaven National Laboratory, was supported by the US Department of Energy, Office of Science, Office of Basic Energy Sciences, under contract No. DE-AC02-98CH10886. The Advanced Light Source is supported by the Director, Office of Science, Office of Basic Energy Sciences, of the US Department of Energy under contract No. DE-AC02-

05CH11231. Use of the Advanced Photon Source, an Office of Science User Facility operated for the US Department of Energy (DOE) Office of Science by the Argonne National Laboratory, was supported by the US DOE under contract No. DE-AC02-06CH11357. Use of the Cornell High Energy Synchrotron Source (CHESS) is supported by the National Science Foundation and the National Institutes of Health/National Institute of General Medical Sciences under NSF award DMR-0936384.

## References

- Adilakshmi, T., Bellur, D. L. & Woodson, S. A. (2008). *Nature (London)*, **455**, 1268–1272.
- Adilakshmi, T., Lease, R. A. & Woodson, S. A. (2006b). *Nucleic Acids Res.* **34**, e64.
- Adilakshmi, T., Ramaswamy, P. & Woodson, S. A. (2006a). *J. Mol. Biol.* **351**, 508–519.
- Adilakshmi, T., Soper, S. F. & Woodson, S. A. (2009). *Methods Enzymol.* **468**, 239–258.
- Angel, T. E., Gupta, S., Jastrzebska, B., Palczewski, K. & Chance, M. R. (2009). *Proc. Natl Acad. Sci. USA*, **106**, 14367–14372.
- Bohon, J., Jennings, L. D., Phillips, C. M., Licht, S. & Chance, M. R. (2008). *Structure*, **16**, 1157–1165.
- Brenowitz, M., Chance, M. R., Dhavan, G. & Takamoto, K. (2002). *Curr. Opin. Struct. Biol.* **12**, 648–653.
- Brenowitz, M., Erie, D. A. & Chance, M. R. (2005). *Proc. Natl Acad. Sci. USA*, **102**, 4659–4660.
- Chaudhuri, B. N., Gupta, S., Urban, V. S., Chance, M. R., D’Mello, R., Smith, L., Lyons, K. & Gee, J. (2011). *Biochemistry*, **50**, 1799–1807.
- Deras, M. L., Brenowitz, M., Ralston, C. Y., Chance, M. R. & Woodson, S. A. (2000). *Biochemistry*, **39**, 10975–10985.
- Dhavan, G. M., Crothers, D. M., Chance, M. R. & Brenowitz, M. (2002). *J. Mol. Biol.* **315**, 1027–1037.
- Guan, J. Q., Almo, S. C. & Chance, M. R. (2004). *Acc. Chem. Res.* **37**, 221–229.
- Guan, J. Q., Takamoto, K., Almo, S. C., Reisler, E. & Chance, M. R. (2005). *Biochemistry*, **44**, 3166–3175.
- Gupta, S., Bavro, V. N., D’Mello, R., Tucker, S. J., Vénien-Bryan, C. & Chance, M. R. (2010). *Structure*, **18**, 839–846.
- Gupta, S., D’Mello, R. & Chance, M. R. (2012). *Proc. Natl Acad. Sci. USA*, **109**, 14882–14887.
- Gupta, S., Sullivan, M., Toomey, J., Kiselar, J. & Chance, M. R. (2007). *J. Synchrotron Rad.* **14**, 233–243.
- Jennings, L. D., Bohon, J., Chance, M. R. & Licht, S. (2008). *Biochemistry*, **47**, 11031–11040.
- Kamal, J. K., Benchaar, S. A., Takamoto, K., Reisler, E. & Chance, M. R. (2007). *Proc. Natl Acad. Sci. USA*, **104**, 7910–7915.
- Kamal, J. K. & Chance, M. R. (2008). *Protein Sci.* **17**, 79–94.
- Kiselar, J. G., Janmey, P. A., Almo, S. C. & Chance, M. R. (2003a). *Mol. Cell. Proteomics*, **2**, 1120–1132.
- Kiselar, J. G., Janmey, P. A., Almo, S. C. & Chance, M. R. (2003b). *Proc. Natl Acad. Sci. USA*, **100**, 3942–3947.
- Kiselar, J. G., Mahaffy, R., Pollard, T. D., Almo, S. C. & Chance, M. R. (2007). *Proc. Natl Acad. Sci. USA*, **104**, 1552–1557.
- Kiselar, J. G., Maleknia, S. D., Sullivan, M., Downard, K. M. & Chance, M. R. (2002). *Int. J. Radiat. Biol.* **78**, 101–114.
- Maleknia, S. D., Brenowitz, M. & Chance, M. R. (1999). *Anal. Chem.* **71**, 3965–3973.
- Nguyenle, T., Laurberg, M., Brenowitz, M. & Noller, H. F. (2006). *J. Mol. Biol.* **359**, 1235–1248.
- Ralston, C. Y., Sclavi, B., Sullivan, M., Deras, M. L., Woodson, S. A., Chance, M. R. & Brenowitz, M. (2000). *Methods Enzymol.* **317**, 353–368.
- Sclavi, B., Sullivan, M., Chance, M. R., Brenowitz, M. & Woodson, S. A. (1998a). *Science*, **279**, 1940–1943.
- Sclavi, B., Woodson, S., Sullivan, M., Chance, M. R. & Brenowitz, M. (1997). *J. Mol. Biol.* **266**, 144–159.
- Sclavi, B., Woodson, S., Sullivan, M., Chance, M. & Brenowitz, M. (1998b). *Methods Enzymol.* **295**, 379–402.
- Shcherbakova, I., Gupta, S., Chance, M. R. & Brenowitz, M. (2004). *J. Mol. Biol.* **342**, 1431–1442.
- Shi, W., Bohon, J., Han, D. P., Habte, H., Qin, Y., Cho, M. W. & Chance, M. R. (2010). *J. Biol. Chem.* **285**, 24290–24298.
- Sullivan, M. R., Rekhi, S., Bohon, J., Gupta, S., Abel, D., Toomey, J. & Chance, M. R. (2008). *Rev. Sci. Instrum.* **79**, 025101.
- Takamoto, K. & Chance, M. R. (2006). *Annu. Rev. Biophys. Biomol. Struct.* **35**, 251–276.
- Takamoto, K., Kamal, J. K. & Chance, M. R. (2007). *Structure*, **15**, 39–51.
- Uchida, T., Takamoto, K., He, Q., Chance, M. R. & Brenowitz, M. (2003). *J. Mol. Biol.* **328**, 463–478.
- Xu, G. & Chance, M. R. (2007). *Chem. Rev.* **107**, 3514–3543.